

Thermal Conductivity of the Iron-Based Superconductor FeSe : Nodeless Gap with Strong Two-Band Character

P. Bourgeois-Hope,¹ S. Chi,² D. A. Bonn,^{2,3} R. Liang,^{2,3} W. N. Hardy,^{2,3}
T. Wolf,⁴ C. Meingast,⁴ N. Doiron-Leyraud,¹ and Louis Taillefer^{1,3,*}

¹Département de physique & RQMP, Université de Sherbrooke, Sherbrooke, Québec J1K 2R1, Canada

²Department of Physics & Astronomy, University of British Columbia, Vancouver, British Columbia V6T 1Z1, Canada

³Canadian Institute for Advanced Research, Toronto, Ontario M5G 1Z8, Canada

⁴Institute of Solid State Physics (IFP), Karlsruhe Institute of Technology, D-76021, Karlsruhe, Germany

(Dated: September 27, 2018)

The thermal conductivity κ of the iron-based superconductor FeSe was measured at temperatures down to 50 mK in magnetic fields up to 17 T. In zero magnetic field, the electronic residual linear term in the $T = 0$ limit, κ_0/T , is vanishingly small. Application of a magnetic field H causes no increase in κ_0/T initially. Those two observations show that there are no zero-energy quasiparticles that carry heat and therefore no nodes in the superconducting gap of FeSe. The full field dependence of κ_0/T has the classic shape of a two-band superconductor, such as MgB₂: it rises exponentially at very low field, with a characteristic field $H^* \ll H_{c2}$, and then more slowly up to the upper critical field H_{c2} . This shows that the superconducting gap is very small on one of the pockets in the Fermi surface of FeSe.

PACS numbers: 74.25.Fy, 74.20.Rp, 74.70.Dd

In the family of iron-based superconductors, the simple binary material FeSe has attracted much attention because when made in thin-film form its superconductivity appears to persist up to critical temperatures as high as $T_c \simeq 100$ K [1]. In bulk form, FeSe is unusual in that it undergoes the standard tetragonal-to-orthorhombic structural transition without the usual accompanying antiferromagnetic transition [2, 3]. This raises fundamental questions about the role of magnetism in causing superconductivity and nematicity.

A basic property of any superconductor is its gap function or structure, which is related to the symmetry of its pairing state, yet there is no consensus on the gap structure of FeSe. A thermal conductivity study of non-stoichiometric FeSe_x revealed no nodes in the gap [4]. By contrast, a huge residual linear term at $T \rightarrow 0$ was reported in a subsequent study of thermal conductivity in stoichiometric FeSe [5], viewed as evidence of nodes in the gap. STM measurements detect a V-shaped density of states at low energy [5, 6] and the penetration depth has a nearly linear temperature dependence at low temperature [5], both features interpreted in terms of nodes. Specific heat measurements down to $T = 0.5$ K show that there are low-lying excitations, but the data cannot distinguish clearly between nodes or just a small minimum gap [7]. Calculations for a model where pairing proceeds via spin excitations yield a superconducting gap with accidental nodes on one of the Fermi surface pockets [8].

In this Letter, we investigate the gap structure of pure stoichiometric FeSe using thermal conductivity, a bulk probe of the superconducting gap highly sensitive to the presence or absence of nodes [9]. Measurements were performed on two single crystals, grown by two different groups, and the results are in excellent agreement. We

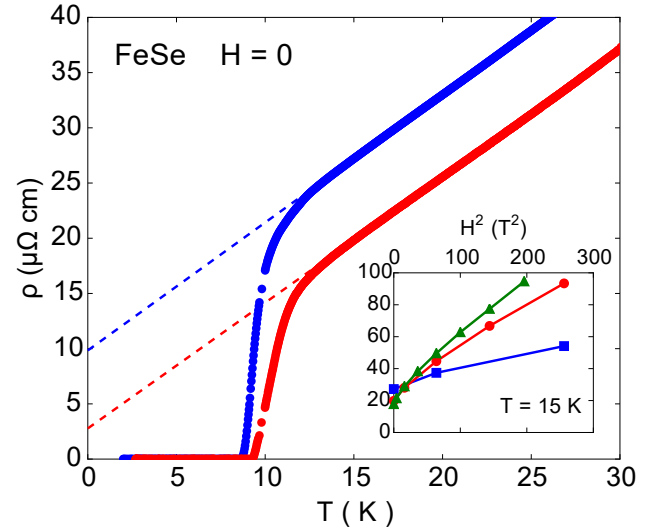


FIG. 1: In-plane electrical resistivity $\rho(T)$ of FeSe for our samples A (red) and B (blue). The dashed lines are a linear fit to $\rho(T)$ between 15 K and 20 K, extended to $T = 0$, giving a residual resistivity $\rho(T \rightarrow 0) = 2.8 \mu\Omega \text{ cm}$ (A) and $9.8 \mu\Omega \text{ cm}$ (B). *Inset*: Dependence of ρ on magnetic field H , at $T = 15$ K, plotted as ρ vs H^2 , for samples A (red circles) and B (blue squares), compared with corresponding data in ref. 5 (green triangles).

find that the residual linear term in $\kappa(T)$ as $T \rightarrow 0$, κ_0/T , is negligible at $H = 0$ and it rises only slowly at first with magnetic field H , clear evidence that there are no nodes in the gap, in contrast with the prior study [5]. However, the field dependence reveals the presence of a very small gap on some part of the Fermi surface, which could account for the low-energy quasiparticle excitations detected in STM and penetration depth.

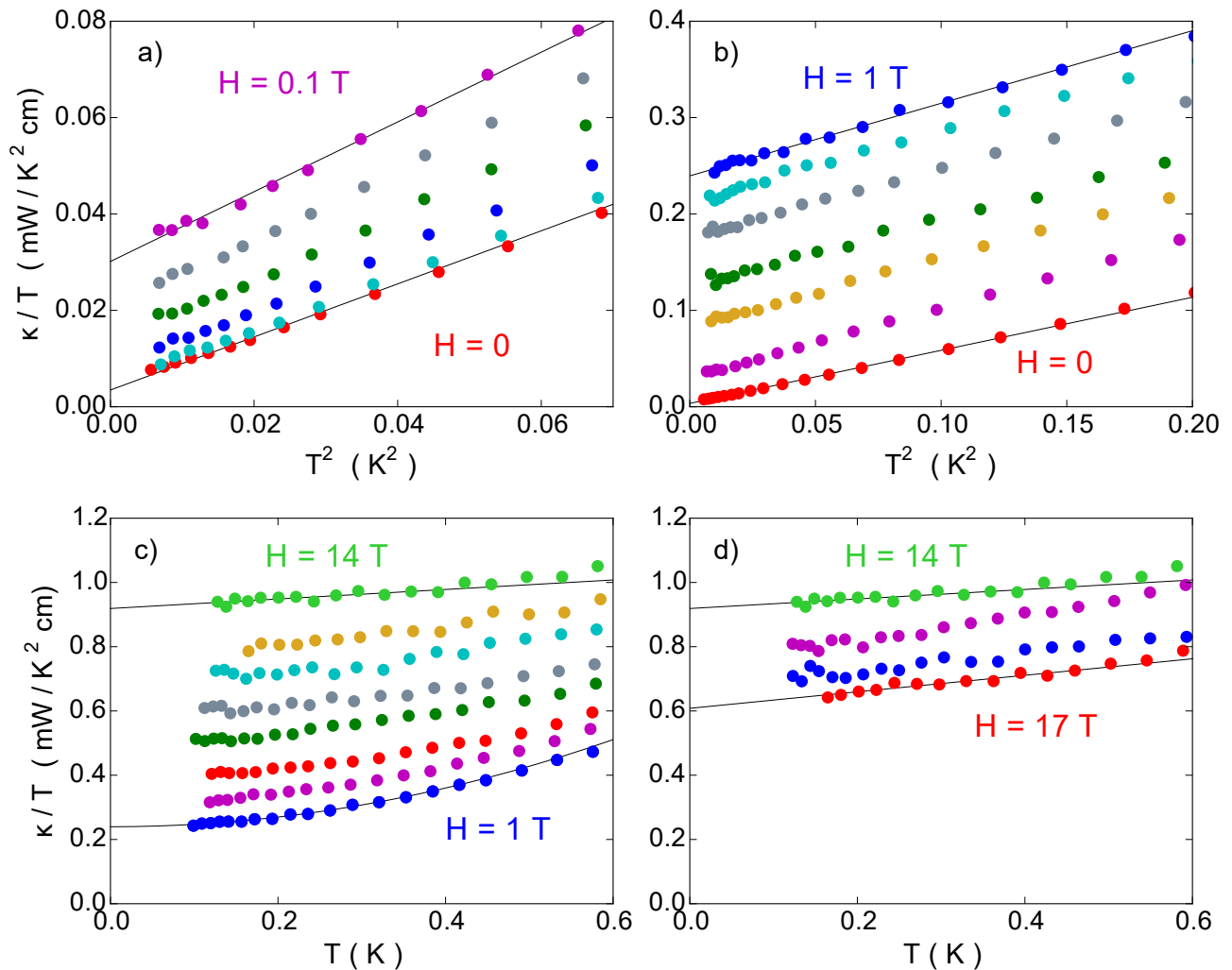


FIG. 2: Temperature dependence of the in-plane thermal conductivity $\kappa(T)$ of FeSe, measured on sample A, with an applied magnetic field $H \parallel c$. (a) Plotted as κ/T vs T^2 for $H = 0, 0.02, 0.04, 0.06, 0.08,$ and 0.1 T (from bottom to top). Lines are a fit to $\kappa/T = a + bT^2$, used to obtain the residual linear term at $T = 0$, $a \equiv \kappa_0/T$. (b) Plotted as κ/T vs T^2 for $H = 0, 0.1, 0.2, 0.3, 0.5, 0.75,$ and 1.0 T (from bottom to top). Lines are a fit to $\kappa/T = a + bT^2$. (c) Plotted as κ/T vs T for $H = 1, 2, 4, 8, 10, 12, 13,$ and 14 T (from bottom to top). The lower line is a fit to $\kappa/T = a + bT^2$ ($H = 1$ T) and the upper line a fit to $\kappa/T = a + bT$ ($H = 14$ T). (d) Plotted as κ/T vs T for $H = 14, 15, 16,$ and 17 T (from top to bottom). Lines are a fit to $\kappa/T = a + bT$. The values of $a \equiv \kappa_0/T$ obtained from a fit to either $\kappa/T = a + bT^2$ ($H < 11$ T) or $\kappa/T = a + bT$ ($H > 11$ T) are plotted as κ_0/T vs H in Fig. 3.

Methods.— Single crystals of FeSe were grown by vapour transport [10]. Sample A was grown at UBC in Vancouver; sample B was grown at KIT in Karlsruhe. They have similar characteristics, but sample A is slightly cleaner, resulting in a slightly higher T_c , namely 9.3 K (A) vs 8.6 K (B) (Fig. 1). The contacts to the sample were made using silver epoxy. The thermal conductivity was measured in a dilution refrigerator down to 50 mK, for a heat current in the basal plane of the orthorhombic crystal structure, as described elsewhere [11]. A magnetic field up to 17 T was applied along the c axis, and always changed at $T > T_c$.

Resistivity.— The in-plane resistivity $\rho(T)$ of our two

samples is in excellent agreement with previously published data [5], when normalized to a common value at $T = 300$ K, namely $\rho(300 \text{ K}) = 410 \mu\Omega \text{ cm}$. Differences are only visible when zooming at low temperature, as done in Fig. 1. We see that the curve for sample B is shifted up relative to that of sample A, so that $\rho(T = 15 \text{ K}) = 20.0 \mu\Omega \text{ cm}$ (A) and $25.5 \mu\Omega \text{ cm}$ (B). For comparison, the sample of FeSe studied in ref. 5 has $T_c \simeq 9.4$ K and $\rho(T = 15 \text{ K}) \simeq 18 \mu\Omega \text{ cm}$, showing that its disorder level is similar to, but slightly lower than that of sample A. A linear extrapolation of $\rho(T)$ to $T = 0$ yields $\rho(T \rightarrow 0) = 2.8 \mu\Omega \text{ cm}$ (A) and $9.8 \mu\Omega \text{ cm}$ (B). This gives a residual resistance ratio

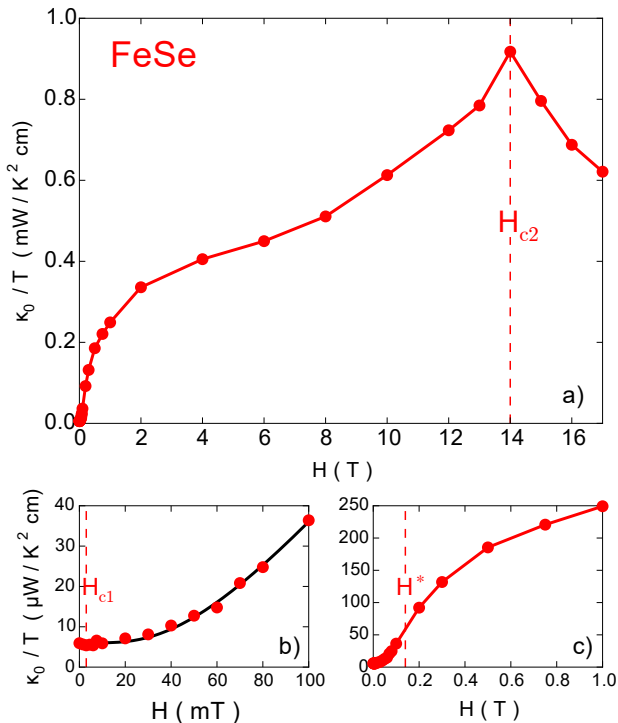


FIG. 3: Field dependence of the residual linear term κ_0/T in FeSe, obtained from fits to the data as in Fig. 2. a) Over the full field range. The vertical dashed line marks the upper critical field, $H_{c2} = 14$ T. b) Zoom below $H = 0.1$ T. The vertical dashed line marks the lower critical field, $H_{c1} = 3$ mT [13]. The full line is an exponential fit to the data up to 0.1 T. c) Zoom below $H = 1.0$ T. The vertical dashed line marks the inflexion point from upward to downward curvature, at $H^* \simeq 150$ mT.

$RRR \equiv \rho(300 \text{ K})/\rho(T \rightarrow 0) = 148$ (A) and 42 (B), a simple dimensionless measure of sample quality. By comparison, the sample of FeSe_x in ref. 4 has $RRR < 10$.

Owing to its semi-metal-like Fermi surface made of small hole-like and electron-like pockets, FeSe displays a strong orbital magnetoresistance (MR) [12], which goes approximately as $\rho(T \rightarrow 0) \propto H^2$. The level of disorder (impurities) is likely to affect the magnitude of the MR, and the cleaner the sample the larger the MR. In the inset of Fig. 1, we compare the MR measured just above T_c (at $T = 15$ K) in our two samples, and that of ref. 5. As expected, the MR increases with increasing RRR, and we see that the sample of ref. 5 is slightly cleaner than our sample A.

Thermal conductivity.—The thermal conductivity $\kappa(T)$ of FeSe at low temperature is shown in the four panels of Fig. 2, for 26 different values of the magnetic field H , ranging from $H = 0$ to $H = 17$ T. Data taken at $H = 1.5, 3.0, 4.5, 6.0, 7.5$ mT are not shown, as they are essentially identical to the data at $H = 0$ and $H = 0.01$ T. At low field ($H < 1.0$ T), the data are well described by the form $\kappa/T = a + bT^2$ below $T \simeq 0.4$ K (Figs. 2a, 2b).

The residual linear term, $a \equiv \kappa_0/T$, is purely electronic, and the second term, bT^2 , is due to phonon conduction [9]. In that regime, phonons are mostly scattered by the sample boundaries, and the phonon mean free path is constant. In this Letter, our focus is entirely on κ_0/T , the electronic transport due to zero-energy quasiparticles. At higher field, $\kappa(T)$ gradually becomes more linear (Fig. 2c), as in the normal state above $H_{c2} = 14$ T (Fig. 2d). In that regime, phonons are predominantly scattered by electrons, and their mean free path goes as $1/T$. Above 10 T, a fit to the form $\kappa/T = a + bT$ below $T \simeq 0.4$ K is used to extract κ_0/T (Figs. 2c, 2d).

At $H = 0$, a fit of the data below 0.4 K to the form $\kappa/T = a + bT^2$ yields a very small value of a , of magnitude $6 \pm 2 \mu\text{W} / \text{K}^2 \text{ cm}$ (Fig. 2a). To put it in perspective, this value should be compared to the value in the normal state, κ_N/T , which we estimate by applying the Wiedemann-Franz law to the residual resistivity $\rho(T \rightarrow 0) = 2.8 \mu\Omega \text{ cm}$ (Fig. 1), giving $\kappa_N/T = (\pi^2/3)(k_B/e)^2/\rho(T \rightarrow 0) = 8.8 \text{ mW} / \text{K}^2 \text{ cm}$. We see that $a = \kappa_0/T$ is less than 0.1 % of the normal state conductivity, a negligible value. This shows that there are no zero-energy quasiparticles in the superconducting state of FeSe at $H = 0$.

Applying a magnetic field is a controlled way of exciting quasiparticles in the superconducting ground state at $T = 0$. Looking at the full H dependence of κ_0/T up to 17 T (Fig. 3a), we see the typical behaviour of a two-band superconductor like MgB_2 [14] or NbSe_2 [15]. Two features are striking. The first is the sharp cusp at $H = 14$ T. This is the upper critical field H_{c2} , below which vortices appear in the sample. The appearance of vortices introduces an additional scattering process, which suddenly curtails the mean free path, causing an abrupt drop in conductivity below H_{c2} , in samples with long electronic mean free path. This happens in any clean type-II superconductor, whether the gap is nodeless – as in Nb or LiFeAs [16] – or nodal – as in KFe_2As_2 [17] or $\text{YBa}_2\text{Cu}_3\text{O}_y$ [18], provided the elastic normal-state mean free path is much longer than the $T = 0$ coherence length ξ (*i.e.* the inter-vortex separation at H_{c2}).

Note that the decrease in κ_0/T above H_{c2} (Fig. 3a) is due to the strong magnetoresistance of the normal state (inset of Fig. 1). As discussed below, the H dependence of κ_0/T is in quantitative agreement with the known H dependence of ρ in the normal state [12]. This proves that the cusp indeed corresponds to the end of the vortex state and it rules out its previous interpretation as an internal phase transition inside the vortex state [5].

The second striking feature of κ_0/T vs H is the rapid rise at low H (Fig. 3a). To investigate this closely, the field was increased in very small steps, starting with $H = 1.5$ mT, then 3.0 mT, and so on (Fig. 3b). In FeSe, the lower critical field above which vortices first enter the sample at $T \rightarrow 0$ is $H_{c1} \simeq 3$ mT [13]. We find that increasing H up to 20 mT, a field 7 times larger

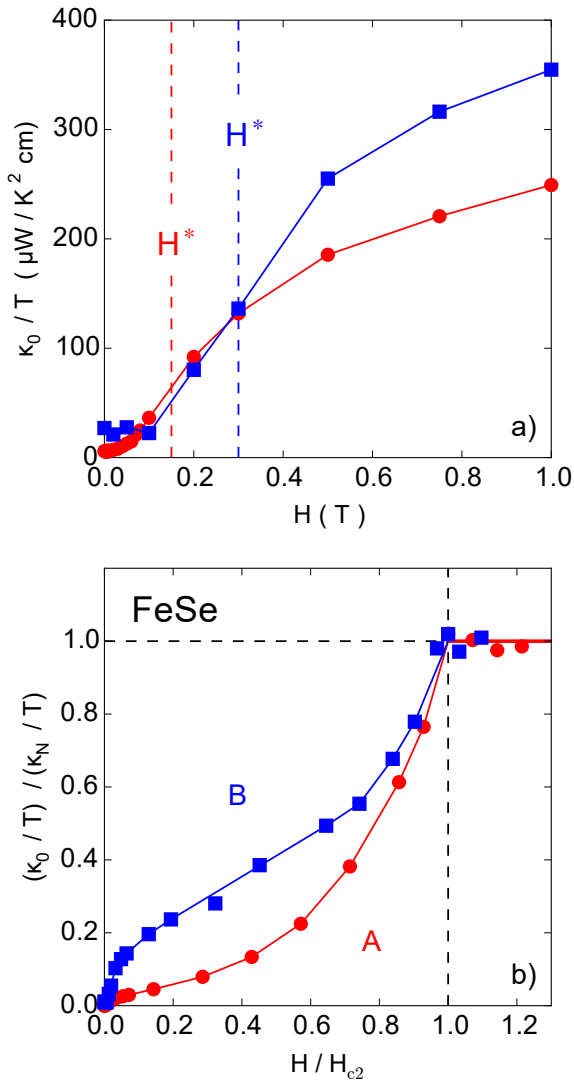


FIG. 4: Field dependence of the residual linear term κ_0/T in FeSe, comparing sample A (red circles) and sample B (blue squares). a) Zoom of the raw data below $H = 1.0$ T. The color-coded vertical dashed lines mark the approximate location of the inflexion point, separating a regime of upward curvature at low H and a regime of downward curvature at higher H , at $H^* \simeq 0.15$ T (red) and $H^* \simeq 0.3$ T (blue). b) Over the full field range, with κ_0/T normalized by the field-dependent normal-state conductivity κ_N/T (see text) and H normalized by H_{c2} .

than H_{c1} , causes no increase in quasiparticle conduction. This confirms that there are no nodes in the gap, for if there were, a field greater than H_{c1} would rapidly excite nodal quasiparticles.

In Fig. 3b, we see that the initial rise in κ_0/T vs H is exponential, so that the field-induced quasiparticle heat conduction in FeSe is an activated process (at low H), very different from the rapid rise characteristic of nodal

superconductors [9]. This shows that there is a minimum gap for quasiparticle excitations, *i.e.* there are no nodes anywhere in the gap structure. However, that minimum gap is much smaller than the maximum gap responsible for setting H_{c2} . Indeed, the characteristic field for the initial rise is roughly $H^* \simeq H_{c2}/100$, if we define H^* as the inflexion point in κ_0/T vs H , where κ_0/T goes from a positive to a negative curvature (Fig. 3c), giving $H^* \simeq 0.15$ T.

The quantity that controls how fast κ_0/T rises with H is not the superconducting gap Δ but the coherence length $\xi \propto v_F/\Delta$, where v_F is the Fermi velocity. In a single-band situation, the upper critical field is set by ξ : $H_{c2} \propto 1/\xi^2 \propto (\Delta/v_F)^2$. In a two-band model, the Fermi surface with the smaller ξ will set H_{c2} , while the surface with the larger ξ will control H^* . In the two-band superconductor MgB₂, $H^* \simeq H_{c2}/10$ because the small gap is 3 times smaller than the large gap [14].

If we accept the interpretation that the Fermi surface of FeSe consists of two distinct pockets – a small Γ -centred hole pocket and a small electron pocket at the corner of the Brillouin zone [5, 19] – with comparable values of v_F [19], then we are forced to conclude that the superconducting gap varies by an order of magnitude around the Fermi surface. There are two scenarios for the k dependence of the gap in FeSe. In the first, the gap is roughly isotropic on both surfaces but much smaller on one of them, *i.e.* $\Delta^* \ll \Delta$. In the second, the gap is highly anisotropic around one of the surfaces, perhaps both, varying from a minimum value Δ_{\min} to a maximum value Δ_{\max} , such that $\Delta_{\min} \ll \Delta_{\max}$. Note that in the iron arsenide Ba_{1-x}K_xFe₂As₂ the superconducting gap acquires a deeper and deeper minimum as the material is more and more underdoped, with x decreasing below $x = 0.4$ (where T_c is maximal) [20]. Of course, it may be that both effects are present in pure FeSe: the gap is smaller *and* anisotropic on one of the two Fermi surfaces. Note that because FeSe is orthorhombic the superconducting gap function will involve a mixture of s -wave and d -wave components, which naturally introduces anisotropy [21].

Effect of disorder. – It is instructive to compare samples with different levels of disorder. In Fig. 4a, we plot κ_0/T vs H , for samples A and B, at fields below $H = 1.0$ T. We see in sample B the same characteristics we saw in sample A, namely a negligible κ_0/T at $H = 0$ ($\simeq 1\%$ of κ_N/T), a flat κ_0/T at low H (in this case up to $H \simeq 100$ mT), and a strong two-band character, with an inflexion point now at $H^* \simeq 0.3$ T. So sample B leads us to the same qualitative conclusions: no nodes, but a very small gap on part of the Fermi surface. Quantitatively, the minimum gap appears to be larger, as measured by the larger value of H^* . It therefore seems that disorder enhances the minimum gap. One way to interpret this effect is for disorder to reduce (or remove) the anisotropy present in the small gap. It

is then conceivable that in samples cleaner than sample A, the anisotropy is such that the deep minima further deepen to produce shallow accidental nodes where the gap changes sign [22]. This is the mechanism proposed by Kasahara and co-workers [5] to explain why they see a large residual κ_0/T in their clean sample of FeSe when no such residual term had been detected in the more disordered FeSe_x [4]. Note, however, that the value of κ_0/T they report at $H = 0$ is enormous [5], 20-40 times larger than the value $\kappa_0/T \simeq 100\text{-}200 \text{ mW} / \text{K}^2 \text{ cm}$ we observe in both our samples just above H^* (Fig. 4a), and a sizeable fraction of the total normal-state conductivity κ_N/T . Their enormous κ_0/T value at $H = 0$ remains a puzzle.

In Fig. 4b, κ_0/T is normalized by the field-dependent normal-state conductivity κ_N/T , and H is normalized by the zero-temperature value of H_{c2} (essentially the same in the two samples). We obtain κ_N/T by fitting the data points above H_{c2} (the 4 data points at $H \geq 14 \text{ T}$ in Fig. 3a, for sample A) to the relation $\kappa_N/T = L_0/(a + bH^2)$, since $\rho = a + bH^2$ in FeSe [12], given that the Wiedemann-Franz law requires that $\kappa_N/T = L_0/\rho$ in the $T = 0$ limit, with $L_0 \equiv (\pi^2/3)(k_B/e)^2$. For sample A, we obtain $b \simeq 50 \text{ n}\Omega \text{ cm} / \text{T}^2$, in excellent agreement with the data of ref. 12 for the normal-state MR of FeSe. In Fig. 4b, we observe a clear shoulder in $(\kappa_0/T) / (\kappa_N/T)$ at $H/H_{c2} \simeq 1/20$, very similar to the shoulder seen in MgB₂ at $H/H_{c2} \simeq 1/9$. In this normalized plot, the two-band character is more apparent for sample B than for sample A. The disorder in sample B is such as to degrade more effectively than in sample A the conductivity of the large-gap Fermi surface relative to that of the small-gap Fermi surface. Our normalized data for κ_0/T vs H on sample B and A (Fig. 4b) can be viewed as cleaner and much cleaner versions of the data in FeSe_x [4], respectively, but they bear no resemblance to the data of ref. [5].

Summary.— In summary, our thermal conductivity measurements on two high-quality crystals of FeSe reveal

a superconducting gap without nodes, but with a strong two-band character, whereby the gap magnitude on one pocket of the Fermi surface of FeSe is an order of magnitude smaller than its magnitude on the other pocket. The presence of such a small gap will make various superconducting properties of FeSe, such as the penetration depth, appear as though they come from a nodal gap, unless measurements are carried out to very low temperature and/or very low energy.

Acknowledgements.— The work at Sherbrooke was supported by a Canada Research Chair, the Canadian Institute for Advanced Research, the National Science and Engineering Research Council of Canada, the Fonds de recherche du Québec - Nature et Technologies, and the Canada Foundation for Innovation.

* E-mail: louis.taillefer@usherbrooke.ca

- [1] J.-F. Ge *et al.*, Nature Materials **14**, 285 (2015).
- [2] M. McQueen *et al.*, Phys. Rev. Lett. **103**, 057002 (2009).
- [3] M. Bendele *et al.*, Phys. Rev. Lett. **104**, 087003 (2010).
- [4] J. K. Dong *et al.*, Phys. Rev. B **80**, 024518 (2009).
- [5] S. Kasahara *et al.*, PNAS **111**, 16309 (2014).
- [6] T. Watashige *et al.*, Phys. Rev. X **5**, 031022 (2015).
- [7] J.-Y. Lin *et al.*, Phys. Rev. B **84**, 220507(R) (2011).
- [8] A. Kreisel *et al.*, Phys. Rev. B **92**, 224515 (2015).
- [9] H. Shakeripour *et al.*, New J. Phys. **11**, 055065 (2009).
- [10] A. E. Boehmer *et al.*, Phys. Rev. B **87**, 180505(R) (2013).
- [11] J. Ph. Reid *et al.*, Phys. Rev. B **82**, 064501 (2010).
- [12] W.D. Watson *et al.*, Phys. Rev. Lett. **115**, 027006 (2015).
- [13] M. Abdel-Hafiez *et al.*, Phys. Rev. B **88**, 174512 (2013).
- [14] A.V. Sologubenko *et al.*, Phys. Rev. B **66**, 014504 (2002).
- [15] E. Boaknin *et al.*, Phys. Rev. Lett. **90**, 117003 (2003).
- [16] M. A. Tanatar *et al.*, Phys. Rev. B **84**, 054507 (2011).
- [17] J. Ph. Reid *et al.*, Phys. Rev. Lett. **109**, 087001 (2012).
- [18] G. Grissonnanche *et al.*, Nat. Commun. **5**, 3280 (2014).
- [19] T. Terashima *et al.*, Phys. Rev. B **90**, 144517 (2014).
- [20] J. Ph. Reid *et al.*, arXiv:1602.03914 (2016).
- [21] J. Kang *et al.*, Phys. Rev. Lett. **113**, 217001 (2014).
- [22] V. Mishra *et al.*, Phys. Rev. B **79**, 094512 (2009).